Cell Calcium 86 (2020) 102137

Contents lists available at ScienceDirect

Cell Calcium

journal homepage: www.elsevier.com/locate/ceca

NCX activity generates spontaneous Ca^{2+} oscillations in the astrocytic leaflet microdomain

László Héja*, Julianna Kardos

Functional Pharmacology Research Group, Institute of Organic Chemistry, Research Centre for Natural Sciences, Hungarian Academy of Sciences, Hungary

ARTICLE INFO

Keywords:
Astrocytic leaflet
Na^+/Ca^{2+} exchange
Ca^{2+} oscillations
Astrocytic Glu-Na^+ symport
Synaptic Glu release
Glu-Na^+ symport

ABSTRACT

The synergy between synaptic Glu release and astrocytic Glu-Na^+ symport is essential to the signalling function of the tripartite synapse. Here we used kinetic data of astrocytic Glu transporters (EAAT) and the Na^+/Ca^{2+} exchanger (NCX) to simulate Glu release, Glu uptake and subsequent Na^+ and Ca^{2+} dynamics in the astrocytic leaflet microdomain following single release event. Model simulations show that Glu-Na^+ symport differently affect intracellular [Na^+] in synapses with different extent of astrocytic coverage. Surprisingly, NCX activity alone has been shown to generate markedly stable, spontaneous Ca^{2+} oscillation in the astrocytic leaflet. These on-going oscillations appear when NCX operates either in the forward or reverse direction. We conjecture that intrinsic NCX activity may play a prominent role in the generation of astrocytic Ca^{2+} oscillations.

1. Introduction

Intracellular high-[K^+]$_i$ and low-[Na^+]$_i$ holds for excitable tissues such as nerve and muscle [1]. Further than nerves, Na^+ transients may activate astrocytes and neuro-glia coupling via uptake of glutamate (Glu) [2–7]. Here we discuss the details of the active astrocytic transport of major excitatory neurotransmitter in the brain, Glu. Similar to neurons, astrocytes also feature complex arborization, comprising of tiny leaflets that are in direct contact with synapses and larger diameter branchlets through which synaptic information can be processed and propagated to the soma. Importantly, these specific microdomains experience highly distinct [Na^+] and [Ca^{2+}] dynamics and it has been recently showed that Glu transporter activation can induce complex Ca^{2+} signalling in leaflets with no contribution from intracellular Ca^{2+} stores [8]. The question now arises as to whether the leaflet, which covers the tripartite synapse [9], is also the seat of the activation of astrocytes and neuro-glia coupling *via* Na^+ and Ca^{2+} transients and oscillations.

With data and concepts already accumulated [4,10–23], we investigated whether Na^+ and Ca^{2+} dynamics in the astrocytic leaflet of tripartite synapse [9,24–26] may interact and collectively contribute to the emergence of complex Ca^{2+} signalling in response to a single synaptic release event. The hypothesis is based on the fact that Glu molecules released from synapse are transported against an electrochemical potential gradient. This involves the symport of 3 Na^+ cations into the cell down the electrochemical potential gradient. The Glu uptake process achieves relatively high [Na^+]$_i$ within the astrocytic leaflet. The high [Na^+]$_i$ possibly will trigger cation exchange by the astrocytic Na^+/Ca^{2+} exchanger NCX. This process performs 3 Na^+: 1 Ca^{2+} stoichiometry.

Simulations of single synaptic Glu release, astrocytic Glu uptake and coupled Na^+ dynamics have been carried out at molecular resolution with different tripartite synapse configurations, i.e. in tightly and loosely wrapped synapses [14]. Model simulations suggest that the synaptic Glu release-associated astrocytic Glu uptake within the astrocytic leaflet highly depends on the morphological arrangement of the leaflet. Surprisingly, the single Glu release-induced Glu-Na^+ symport is only weakly coupled to Na^+-Ca^{2+} exchange dynamics. Importantly, NCX intrinsically generates spontaneous astrocytic Ca^{2+} oscillations.

2. Simulation of interplay between Na^+ and Ca^{2+} dynamics in astrocytic leaflets

2.1. Modelling dynamic coverage of the tripartite synapse by astrocytic leaflets

An important and less recognized feature of the astrocytic control over neuronal activity is the highly variable coverage of synapses by astrocytic leaflets. This astrocytic formation around the synapse establishes the astroglial cradle that protects and controls the synapse throughout its life from synaptogenesis to synapse elimination [27]. Reportedly [28], astrocytes in the cerebellum almost completely wrap

* Corresponding author.
E-mail address: heja.laszlo@ttk.mta.hu (L. Héja).

https://doi.org/10.1016/j.ceca.2019.102137
Received 13 September 2019; Received in revised form 1 December 2019; Accepted 1 December 2019
Available online 05 December 2019

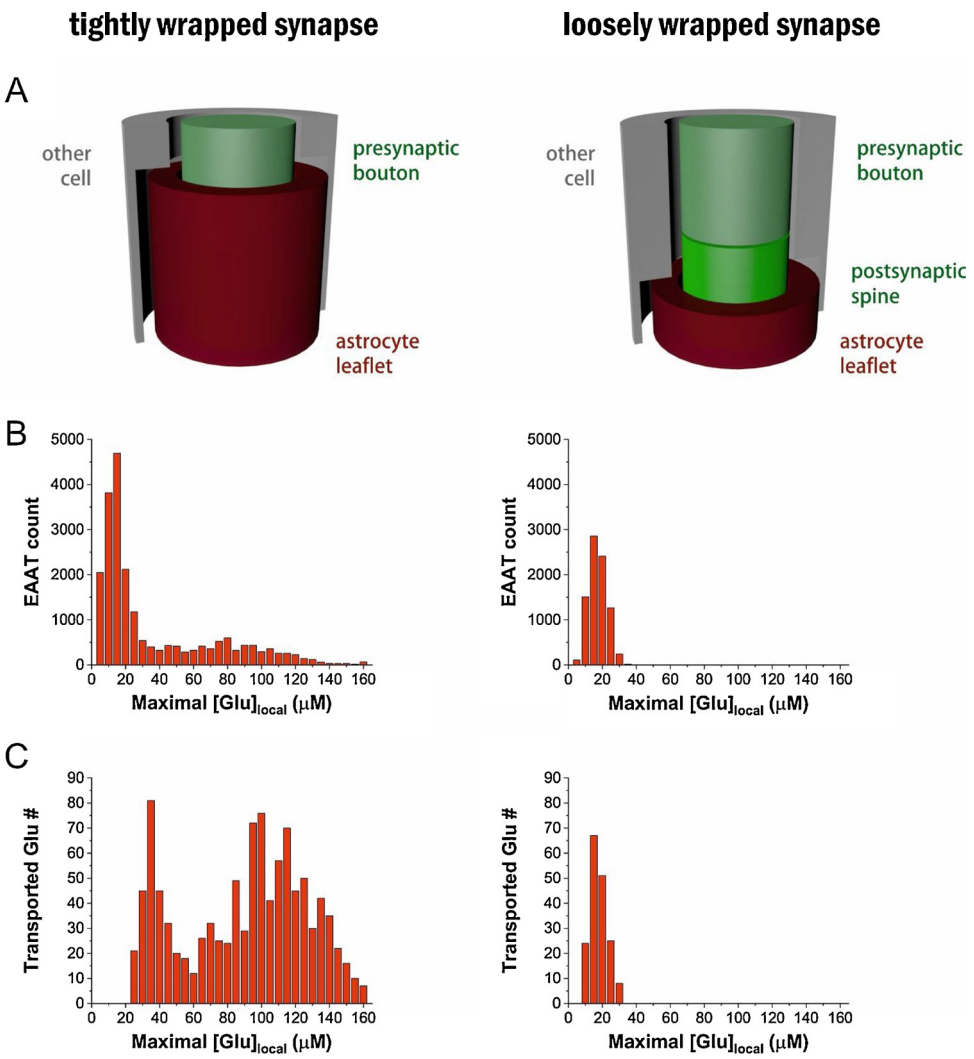

Fig. 1. EAAT subpopulations on the astrocyte leaflet are exposed to different extracellular Glu concentration in the tightly vs. loosely wrapped synapses. A) Model geometry of the tightly (left) and loosely (right) wrapped synapses. B) Distribution of EAAT molecules in the tightly (left) and loosely (right) wrapped synapses based on the maximal local [Glu] in their $50 \times 50 \times 50\,nm^3$ neighborhood. C) Net number of Glu molecules transported by EAATs in the tightly (left) and loosely (right) wrapped synapses based on the maximal local [Glu] in their $50 \times 50 \times 50\,nm^3$ neighborhood. Baseline $[Na^+]_{i,0} = 15$ mM and baseline $[Ca^{2+}]_{i,0} = 100$ nM for all figures.

dendritic spines (74 % coverage), while spines of pyramidal cells in the visual cortex are only partially covered (29 %). In addition, astrocytic coverage of different spine types can also be significantly different in the same hippocampal region [29]. These baseline differences in the astrocytic coverage are further amplified by the remarkable ability of astrocytes to dynamically change leaflet morphology in response to fluctuations in neuronal activity due to stimulation or drug exposure [30,31]. Since Glu uptake and consequently the coupled Na^+ influx is crucially dependent on astrocytic coverage, the tightness of astrocyte wrapping of the synapse can significantly alter the Na^+ dynamics in the leaflet.

To explore the potential impact of different astrocytic coverages of the synapse, we simulated synaptic Glu release-induced intracellular Na^+ and Ca^{2+} dynamics in two different scenarios. In the tightly wrapped synaptic model, astrocytic leaflet completely ensheated the postsynaptic spine and 50 % of the presynaptic bouton. In the loosely wrapped synapse, astrocytic leaflet covered only the 50 % of the spine and did not touch the bouton. In both models (Fig. 1A), the presynaptic and postsynaptic neuronal compartments were considered to have a cylindrical shape with diameter of 400 nm. Height of the synaptic cleft was set to 20 nm. Width of the extracellular space was set to 50 nm, except around the leaflet, where it was set to 20 nm. Width of the leaflet was 100 nm, while its length was set to 600 nm in the tightly wrapped synapse and 200 nm in the loosely wrapped synapse. Ca^{2+} was allowed to freely diffuse in and out of the leaflet to the connecting astrocytic intracellular space allowing steady state $[Ca^{2+}]_i$ after NCX-mediated Ca^{2+} transport.

Importantly, due to its small size, Ca^{2+} stores are not able to enter the leaflet [25,27], which helped us to reduce the complexity of the model, making NCX activity and diffusion the only source and sink of intracellular Ca^{2+}.

2.2. Markovian models of Glu-Na^+ symport and Na^+/Ca^{2+} exchange kinetics

Markovian kinetic models of astrocytic EAATs and NCX were constructed according to published rate constants based on experimental data. Glu uptake by EAATs was modelled by a 13-step cycle comprised of separate bindings and unbindings of 3 Na^+, 1H^+, 1 K^+ and 1 Glu molecule [32]. NCX activity was modelled by a 6-step cycle according to Chu and co-workers [33]. 10800/μm^2 EAAT [34] and 500/μm^2 NCX [33] molecules were distributed randomly on the astrocytic leaflet surface.

Extracellular concentrations of relevant ions ($[Na^+]_e = 140$ mM; $[K^+]_e = 3$ mM; $[Ca^{2+}]_e = 2$ mM) as well as intracellular $[K^+]_i$ (130 mM) and $[Glu]_i$ (3 mM) were kept constant during the simulation. Baseline $[Glu]_e$ (0.3 μM), $[Na^+]_{i,0}$ (5, 10, 15 or 20 mM) and $[Ca^{2+}]_{i,0}$ (50, 100, 200 or 1000 nM) were allowed to change during the simulation due to Glu release, intracellular Ca^{2+} diffusion and activation of EAATs and NCX.

Before starting the simulation, EAATs and NCX randomly populated the available states and allowed to reach steady-state distribution for

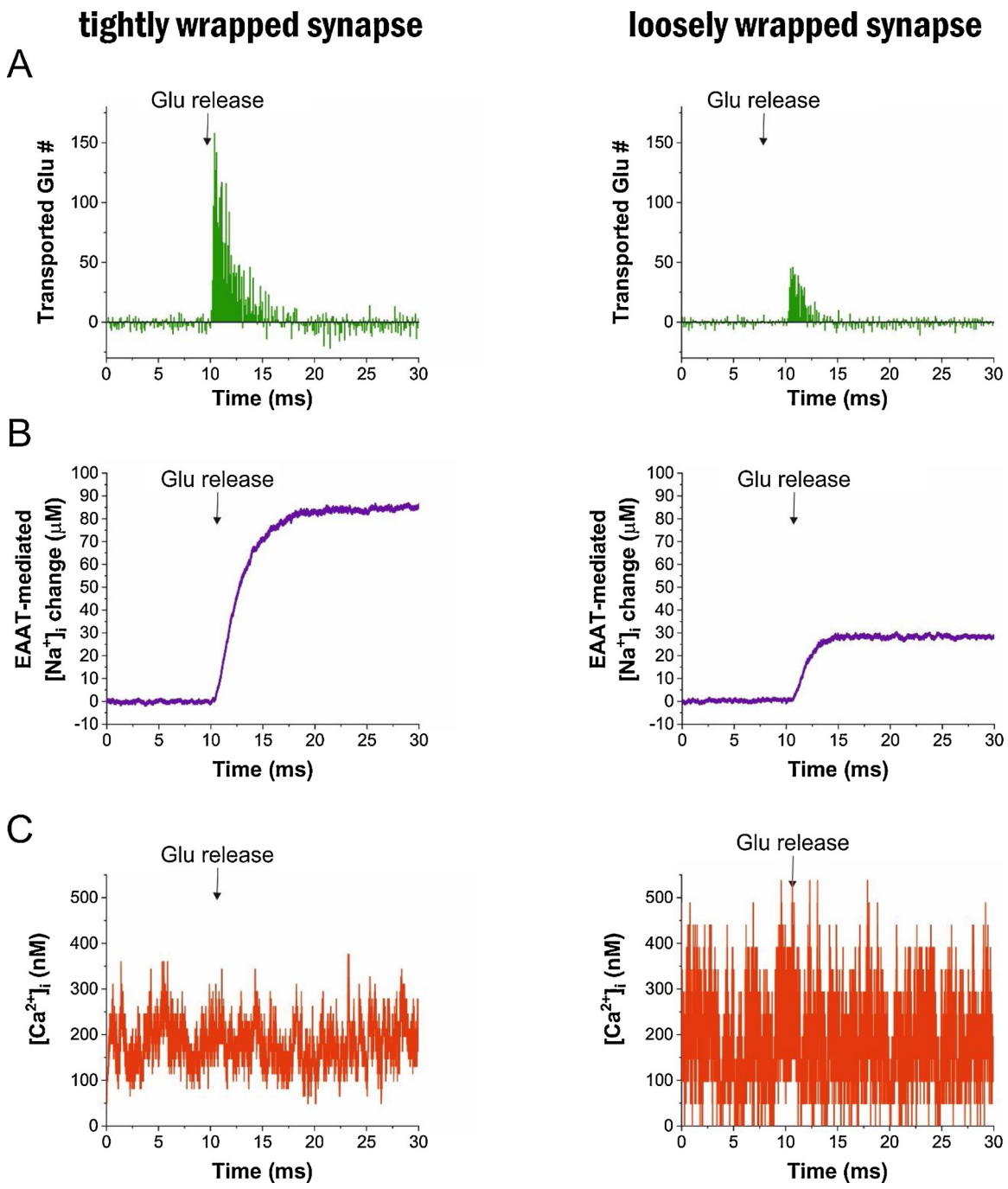

Fig. 2. A) Net number of Glu molecules transported by EAATs following synaptic Glu release in the tightly (left) and loosely (right) wrapped synapse in each 0.1 ms interval. Positive and negative values correspond to net Glu uptake and Glu release, respectively. B) EAAT-mediated changes in $[Na^+]_i$ in astrocyte leaflet in the tightly (left) and loosely (right) wrapped synapses. C) NCX-mediated changes in $[Ca^{2+}]_i$ in astrocyte leaflet in the tightly (left) and loosely (right) wrapped synapse. NCX activity intrinsically produces intracellular $[Ca^{2+}]$ oscillation in both models. Tightly wrapped synapse: $V_{leaflet} = 0.11\ \mu m^3$, influx of 1 Ca^{2+} ion corresponds to $\Delta[Ca^{2+}]_i = 16$ nM. Loosely wrapped synapse: $V_{leaflet} = 0.034\ \mu m^3$, influx of 1 Ca^{2+} ion corresponds to $\Delta[Ca^{2+}]_i = 49$ nM. Baseline $[Na^+]_{i,0} = 15$ mM and baseline $[Ca^{2+}]_{i,0} = 100$ nM for all figures.

30 ms at the above concentrations. Simulations begun with a further 10 ms baseline activity before initiating single synaptic Glu release.

2.3. Glu release and diffusion

Instantaneous release of 5000 Glu molecules was triggered at the center of the presynaptic bouton after 10 ms. Diffusion of independent Glu molecules in the 3D extracellular space was estimated by random walks at 1 μs intervals. Diffusion coefficient of Glu was set to 0.33 μm^2/ms [25].

2.4. Electrogenic Glu-Na^+ symport

Importantly, transitions of EAAT states in the transport cycle were determined based on the local [Glu] in the surrounding $50 \times 50 \times 50\ nm^3$ extracellular microdomain of each EAAT molecule, instead of the average extracellular [Glu]. This feature of our simulation allowed us to take into account the highly variable and dynamically changing extracellular [Glu] following Glu release.

We found that there is a remarkable difference in the extracellular Glu concentration near the EAAT molecules in the tightly vs. loosely

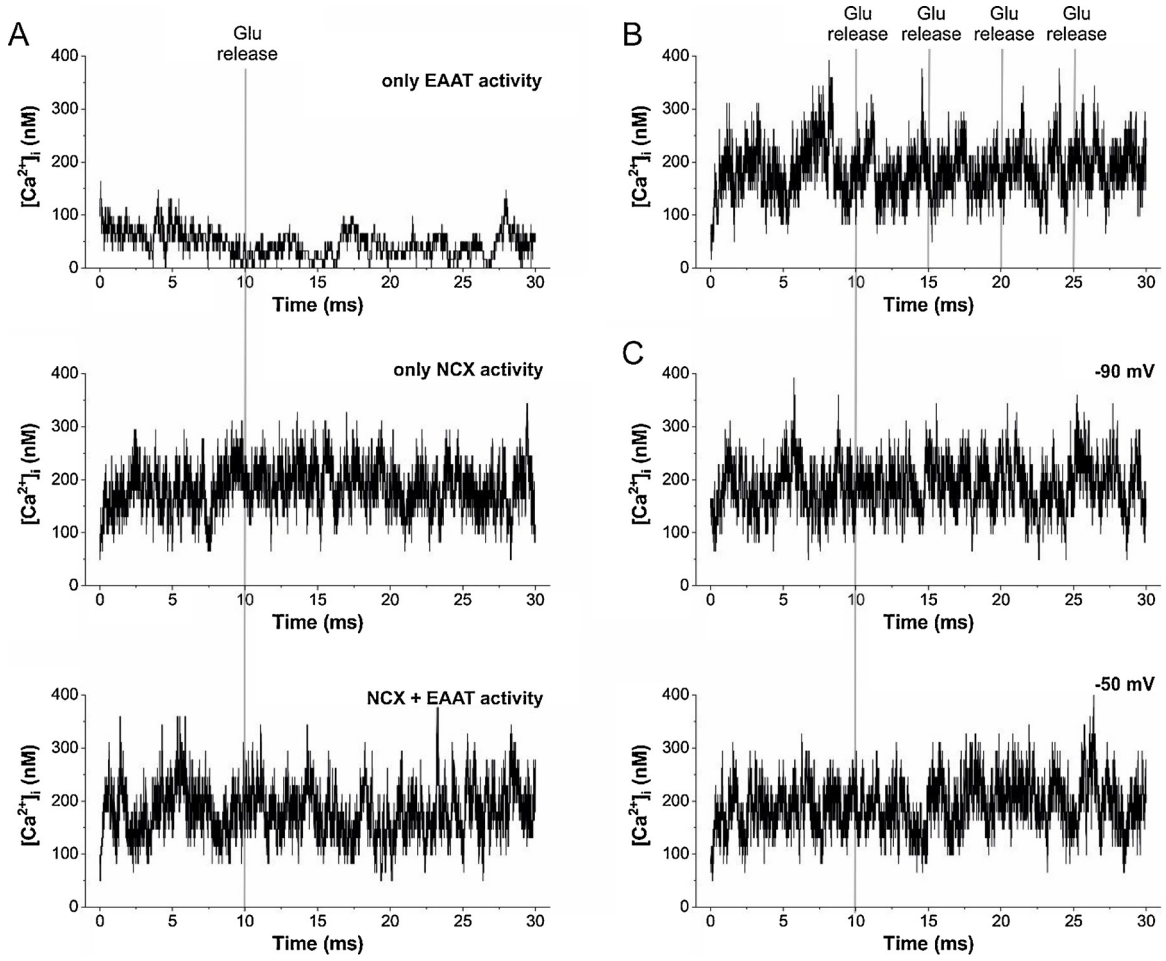

Fig. 3. NCX activity is necessary and sufficient to generate $[Ca^{2+}]_i$ oscillation in the astrocyte leaflet. A) $[Ca^{2+}]_i$ in astrocyte leaflet in the tightly wrapped synapse with EAAT and/or NCX activity. (Top) EAAT activity alone does not induce rhythmic $[Ca^{2+}]_i$ changes. (Middle) NCX activity alone is sufficient to generate $[Ca^{2+}]_i$ oscillation. (Bottom) The NCX-generated $[Ca^{2+}]_i$ oscillation is not modulated by EAAT function. B) High-frequency (200 Hz) firing of the presynaptic neuron does not significantly affect NCX-generated $[Ca^{2+}]_i$ oscillation. Both EAAT and NCX activities were considered. C) NCX-generated $[Ca^{2+}]_i$ oscillation is not affected by changing the astroglial membrane potential to −90 mV (top) or −50 mV (bottom). Both EAAT and NCX activities were considered. Baseline $[Ca^{2+}]_{i,0}$ = 100 nM, baseline $[Na^+]_{i,0}$ = 15 mM in all simulations. Tightly wrapped synapse $V_{leaflet}$ = 0.11 μm^3, influx of 1 Ca^{2+} ion corresponds to $\Delta[Ca^{2+}]_i$ = 16 nM.

wrapped synapses. Based on the local [Glu], two subpopulations of EAATs can be clearly distinguished in the tightly wrapped synapse (Fig. 1B). Approximately half of the EAAT molecules experience a relatively low and invariable Glu concentration (0–30 μM), while the other half is exposed to 5 times higher extracellular [Glu] (40–150 μM). Importantly, this high-[Glu] exposed population is responsible for the majority of Glu uptake (Fig. 1C).

In the loosely wrapped synapse in which the astrocyte leaflet is withdrawn from the synaptic cleft, this highly active EAAT subpopulation is missing (Fig. 1B and C), assuming largely different ion dynamics in the intracellular space.

2.5. Na^+ and Ca^{2+} dynamics in the astrocyte leaflet following Glu release

Astroglial Na^+ dynamics is considered to be a prominent mechanism by which astrocytic functions, like Glu, GABA and glycine transport are coupled to each other and also to neuronal activity [16,35]. Perturbations in intracellular astrocytic $[Na^+]$, due to the function of the above transporters are compensated by Na^+/K^+ ATPase and other plasmamembrane proteins. Therefore, astrocytes, and especially the synapse-facing microdomains experience complex Na^+ signaling [36]which is also coupled to Ca^{2+} signalling through NCX.

According to our simulation, following a single synaptic release event, approximately 46 % of the released Glu molecules are taken up by the astrocyte leaflet (Fig. 2A), causing a moderate increase in the intracellular $[Na^+]$ (Fig. 2B). Noteworthy, it is widely believed that due to the high expression level of glial Glu transporters and their 3 Na^+ : 1 Glu stoichiometry, EAAT activation substantially increases the astrocytic $[Na^+]_i$. However, even the tiny volume of the astrocytic leaflet (0.102 μm^3 in our tightly wrapped synapse model) contains approximately 920000 Na^+ ions (corresponding to 15 mM), therefore the ~2300 Glu molecules transported after a single release event can only slightly contribute to the intracellular $[Na^+]$.

2.6. NCX activity generates stable astrocytic Ca^{2+} oscillation

Despite the subtle $[Na^+]$ increase outlined above, it may still be expected to reverse the Na^+/Ca^{2+} exchanger (NCX), because it is known to operate close to its reversal potential. According to our simulation, however, a single release event is not sufficient to completely reverse NCX. Surprisingly, however, NCX activity intrinsically induce an intracellular Ca^{2+} oscillation, regardless of any other secondary Na^+ or Ca^{2+} transport processes (Fig. 2C). To characterize the mechanism behind this emerging $[Ca^{2+}]$ oscillation, we first modelled how diffusion alone changes $[Ca^{2+}]_i$ (Fig. 3A, top). Under this condition, only low amplitude, irregular fluctuations could be observed. Since NCX was "disabled" in this simulation, as expected, EAAT activity did not modulate the $[Ca^{2+}]_i$ profile. In contrast, introduction of NCX (Fig. 3A,

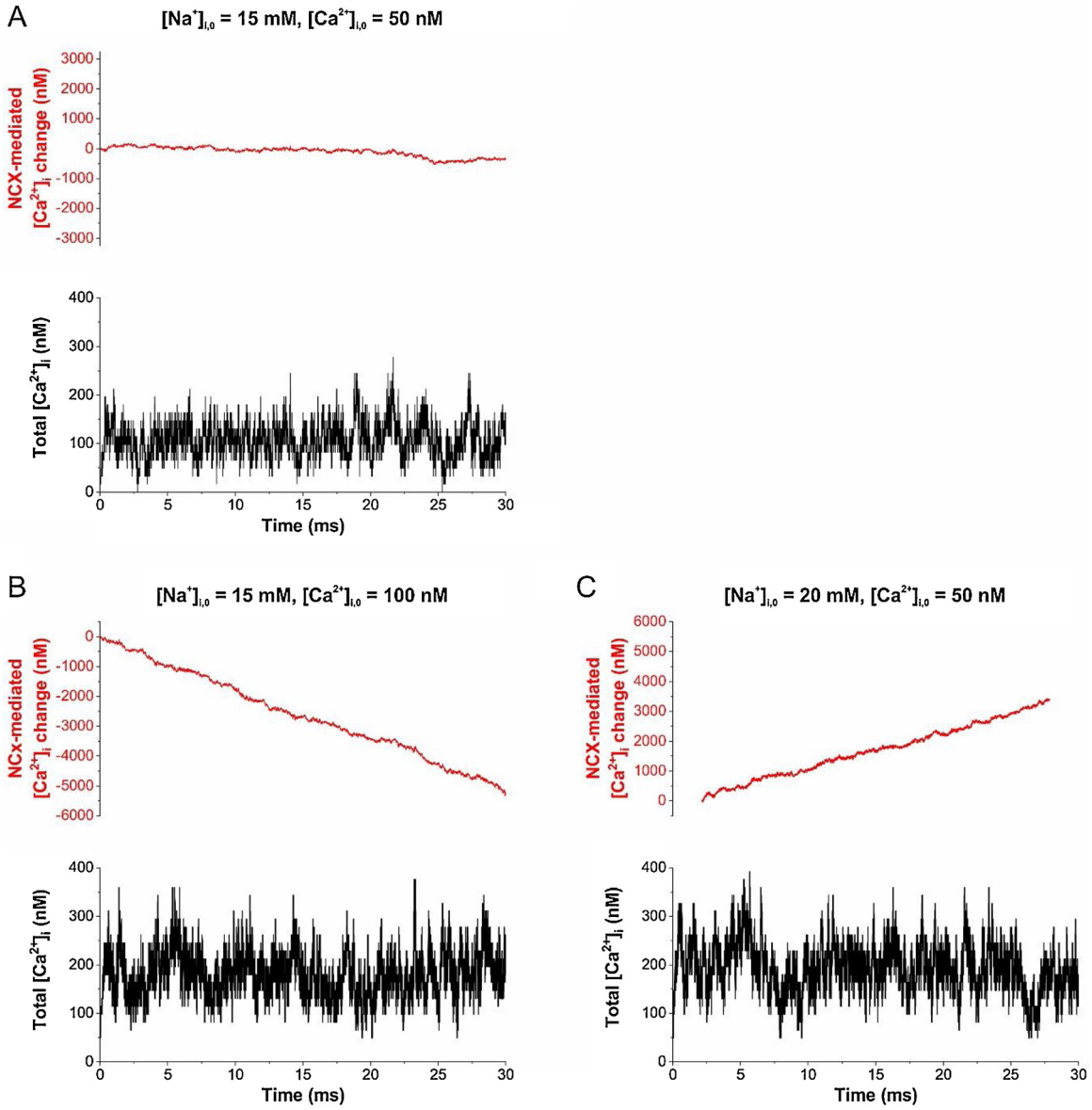

Fig. 4. Spontaneous Ca^{2+} oscillations appear during both forward and reverse operation of NCX. Number of Ca^{2+} ions bound to (negative values) and dissociated from (positive values) NCX are shown (top). The changes in intracellular $[Ca^{2+}]$, taking into account the diffusion as well is shown in the bottom. Spontaneous Ca^{2+} oscillations can be observed when NCX operates near to equilibrium (A), operating in the reverse (B) or forward (C) mode, depending on the intracellular baseline $[Ca^{2+}]_i$ and $[Na^+]_i$. Tightly wrapped synapse $V_{leaflet}$ = 0.11 μm^3, influx of 1 Ca^{2+} ion corresponds to $\Delta[Ca^{2+}]_i$ = 16 nM.

middle) generated a high-amplitude oscillation which was still not affected by Glu release, even when EAATs were also present (Fig. 3A, bottom). Therefore, intrinsic NCX activity is sufficient to generate astrocytic $[Ca^{2+}]$ oscillation. Since single release event resulted only in a slightly elevated astrocytic $[Na^+]_i$, we also simulated an intense excitation. However, even a high-frequency (200 Hz) synaptic release was not able to modulate the NCX-mediated $[Ca^{2+}]$ oscillation (Fig. 3B). The oscillation was also not affected by changing the astrocytic resting membrane potential to either −90 or −50 mV from the initial −70 mV (Fig. 3C). In summary, NCX activity is sufficient to generate a remarkably stable, spontaneous $[Ca^{2+}]$ oscillation in the astrocytic leaflet, which is maintained even without any Glu release event.

After recognizing the stability of NCX-mediated intracellular $[Ca^{2+}]$ oscillations, we also investigated whether it appears during forward or reverse operation of the transporter. Simulations were run under 3 distinct conditions. Setting intracellular $[Na^+]$ and $[Ca^{2+}]$ to 15 mM and 50 nM, respectively, nearly equilibrates NCX. Elevating $[Ca^{2+}]_i$ to 100 nM triggers robust forward operation, pumping out Ca^{2+} from the cell, while increasing $[Na^+]_i$ to 20 mM reverses the transporter. These data also highlight that NCX may be very sensitive to changes in the astrocytic $[Na^+]_i$ which is determined in the 15–20 mM range. Surprisingly, Ca^{2+} oscillations appeared in all three scenarios (Fig. 4), suggesting that temporal fluctuations in the NCX transport cycle can be sufficient to induce Ca^{2+} oscillations irrespective of the overall operation direction of the transporter. The sustained spontaneous Ca^{2+} oscillation in the astrocytic leaflet does not necessarily involve Ca^{2+} translocation through the membrane, but may be associated with the molecular mechanisms of NCX action kinetics [32], namely transitions between empty and calcium-bound states of the inward-facing NCX.

Based on the above data, we hypothesize that NCX activity may lie behind the appearance of astrocytic Ca^{2+} oscillations. Importantly, it has been shown that Ca^{2+} fluctuations in thin astrocytic processes are preserved in IP_3 type 2 receptor (IP3R2) knock-out animals [37], suggesting that local Ca^{2+} oscillations are not driven by store-operated mechanisms. We conjecture that it is the intrinsic NCX activity that maintains this signalling. In addition, spreading of this local Ca^{2+}

fluctuation to larger processes may provide the triggering oscillatory signal which (when amplified by calcium stores) can induce macroscopically detectable Ca^{2+} oscillations in larger scales or even in astrocyte networks.

3. Pathophysiological implications

The Glu-uptake induced activation of Na^+ dynamics in astrocytes discussed in this paper represents only local players of an extensive network of the tripartite synapse, the focal point in neuro-glia coupling [2–7]. We and others increasingly recognized the role of potential interplay of Glu-uptake and other Na^+-dependent transport processes as contributing factors in various diseases, such as Huntington, Alzheimer, Tourette, epilepsy, stroke, demyelinating diseases, hyperammonemia, cardiac ischemia and cancer [2,14,38–52].

As outlined above, NCX is intrinsically able to generate Ca^{2+} oscillations in the astrocytic leaflet and this oscillatory activity is remarkably stable across widely different intracellular Na^+ and Ca^{2+} concentrations, membrane potentials, synaptic firing rates and NCX operation directions. Furthering neuron-glia interactions, these functions shall strengthen signalling close by the tripartite synapse. Possibly, we may associate a range of prokaryotic/eukaryotic cell- and isoform/splice variant-specific NCX transport cycles (0.5 s^{-1} to 2500 s^{-1}) [23] to a variety of synaptic strengths. Amplification of this local fluctuation by Ca^{2+} stores in the connecting larger astrocytic processes and the resulting large-scale Ca^{2+} signalling could affect the extensive network of tripartite synapses and pertinent astrocytic signalling throughout brain areas [2,7,13,14,53–60].

CRediT authorship contribution statement

László Héja: Conceptualization, Data curation, Formal analysis, Funding acquisition, Methodology, Software, Supervision, Validation, Visualization, Writing - original draft, Writing - review & editing. **Julianna Kardos:** Conceptualization, Investigation, Methodology, Supervision, Writing - original draft, Writing - review & editing.

Acknowledgements

This work was supported by grants VEKOP-2.1.1-15-2016-00156 and National Research, Development and Innovation Office grant OTKA K124558.

References

[1] A.K. Solomon, Ion transport in single cell populations, Biophys. J. 2 (1962) 79–95.
[2] J. Kardos, L. Héja, K. Jemnitz, R. Kovács, M. Palkovits, The nature of early astroglial protection - fast activation and signaling, Prog. Neurobiol. 153 (2017) 86–99.
[3] I.E. Polykretis, V. Ivanov, K.P. Michmizos, A Neural-astrocytic Network Architecture: Astrocytic Calcium Waves Modulate Synchronous Neuronal Activity, (2019) arXiv:1807.02514 [q-bio.NC]N.
[4] A. Semyanov, Spatiotemporal pattern of calcium activity in astrocytic network, Cell Calcium 78 (2019) 15–25.
[5] C.R. Rose, L. Felix, A. Zeug, D. Dietrich, A. Reiner, C. Henneberger, Astroglial glutamate signaling and uptake in the hippocampus, Front. Mol. Neurosci. 10 (2018) 451.
[6] Z. Szabó, G. Héja, O. Szalay, A. Kékesi, K. Füredi, K. Szebényi, Á. Dobolyi, T.I. Orbán, O. Kolacsek, T. Tompa, Z. Miskolczy, L. Biczók, B. Rózsa, B. Sarkadi, J. Kardos, Extensive astrocyte synchronization advances neuronal coupling in slow wave activity in vivo, Sci. Rep. 7 (2017) 6018.
[7] A. Verkhratsky, M. Nedergaard, Physiology of astroglia, Physiol. Rev. 98 (2018) 239–389.
[8] J.J. Wade, K. Breslin, K. Wong-Lin, J. Harkin, B. Flanagan, H. Van Zalinge, S. Hall, M. Dallas, A. Bithell, A. Verkhratsky, L. McDaid, Calcium microdomain formation at the perisynaptic cradle due to NCX reversal: a computational study, Front. Cell. Neurosci. 13 (2019) 185.
[9] Araque, V. Parpura, R.P. Sanzgiri, P.G. Haydon, Tripartite synapses: glia, the unacknowledged partner, Trends Neurosci. 22 (1999) 208–215.
[10] M.P. Blaustein, W.J. Lederer, Sodium/calcium exchange: its physiological implications, Physiol. Rev. 79 (1999) 763–854.
[11] A.R. Brazhe, A.Y. Verisokin, D.V. Verveyko, D.E. Postnov, Sodium-Calcium exchanger can account for regenerative Ca^{2+} entry in thin astrocyte processes, Front. Cell. Neurosci. 12 (1918) art. 250.
[12] K. Breslin, J.J. Wade, K. Wong-Lin, J. Harkin, B. Flanagan, H. Van Zalinge, S. Hall, M. Walker, A. Verkhratsky, L. McDaid, Potassium and sodium microdomains in thin astroglial processes: a computational model study, PLoS Comput. Biol. 14 (2018) e1006151, , https://doi.org/10.1371/journal.pcbi.1006151.
[13] L. Héja, G. Nyitrai, O. Kékesi, A. Dobolyi, P. Szabó, R. Fiath, I. Ulbert, B. Pál-Szenthe, M. Palkovits, J. Kardos, Astrocytes convert network excitation to tonic inhibition of neurons, BMC Biol. 10 (2012) 26.
[14] L. Héja, Á. Simon, Z. Szabó, J. Kardos, Feedback adaptation of synaptic excitability via Glu: Na^+ symport driven astrocytic GABA and Gln release, Neuropharmacology (2019), https://doi.org/10.1016/j.neuropharm.2019.05.006.
[15] D. Khananshvili, Sodium-calcium exchangers (NCX): molecular hallmarks underlying the tissue-specific and systemic functions, Plügers Archiv. 466 (2014) 43–60.
[16] S. Kirischuk, L. Héja, J. Kardos, B. Billups, Astrocyte sodium signaling and the regulation of neurotransmission, Glia 64 (2016) 1655–1666.
[17] V. Matyash, H. Kettenmann, Heterogeneity in astrocyte morphology and physiology, Brain Res. Rev. 63 (2010) 2–10.
[18] V. Lariccia, S. Amoroso, Calcium- and ATP-dependent regulation of Na/Ca exchange function in BHK cells: comparison of NCX1 and NCX3 exchangers, Cell Calcium 73 (2018) 95–103.
[19] S. Oh, O. Boudker, Kinetic mechanism of coupled binding in sodium-aspartate symporter GltPh, Elife 7 (2018) e37291.
[20] Reyes, C. Ginter, O. Boudker, Transport mechanism of a bacterial homologue of glutamate transporters, Nature 462 (2009) 880–885.
[21] C.R. Rose, B.R. Ransom, Intracellular sodium homeostasis in rat hippocampal astrocytes, J. Physiol. 491 (1996) 291–305.
[22] E. Shigetomi, E.A. Bushong, M.D. Haustein, X. Tong, O. Jackson-Weaver, S. Kracun, J. Xu, M.V. Sofroniew, M.H. Ellisman, B.S. Khakh, Imaging calcium microdomains within entire astrocyte territories and endfeet with GCaMPs expressed using adeno-associated viruses, J. Gen. Physiol. 141 (2013) 633–647.
[23] L. van Dijk, M. Giladi, B. Refaeli, R. Hiller, M.H. Cheng, I. Bahar, D. Khananshvilii, Key residues controlling bidirectional ion movements in Na^+/Ca^{2+} exchanger, Cell Calcium 76 (2018) 10–22.
[24] A. Denizot, M. Arizono, U.V. Nägerl, H. Soula, H. Berry, Simulation of calcium signaling in fine astrocytic processes: effect of spatial properties on spontaneous activity, Cold Spring Harbor Labor. (2019), https://doi.org/10.1101/567388.
[25] N. Gavrilov, I. Golyagina, A. Brazhe, A. Scimemi, V. Turlapov, A. Semyanov, Astrocytic coverage of dendritic spines, dendritic shafts, and axonal boutons in hippocampal neuropil, Front. Cell. Neurosci. 12 (2018) 248.
[26] L.P. Savtchenko, L. Bard, T.P. Jensen, J.P. Reynolds, I. Kraev, N. Medvedev, M.G. Stewart, C. Henneberger, D.A. Rusakov, Disentangling astroglial physiology with a realistic cell model in silico, Nat. Commun. 9 (2018) 3554.
[27] A. Verkhratsky, M. Nedergaard, Astroglial cradle in the life of the synapse, Philos. Trans. R. Soc. Lond., B, Biol. Sci. 369 (2014) 20130595.
[28] J. Spacek, Three-dimensional analysis of dendritic spines. III. Glial sheath, Anat. Embryol (Berl) 171 (1985) 245–252.
[29] N. Medvedev, V. Popov, C. Henneberger, I. Kraev, D.A. Rusakov, M.G. Stewart, Glia selectively approach synapses on thin dendritic spines, Philos. Trans. R. Soc. Lond. B Biol. Sci. 369 (2014) 20140047.
[30] D.T. Theodosis, D.A. Poulain, S.H. Oliet, Activity-dependent structural and functional plasticity of astrocyte-neuron interactions, Physiol. Rev. 88 (2008) 983–1008.
[31] Perez-Alvarez, M. Navarrete, A. Covelo, E.D. Martin, A. Araque, Structural and functional plasticity of astrocyte processes and dendritic spine interactions, J. Neurosci. 34 (2014) 12738–12744.
[32] D.E. Bergles, A.V. Tzingounis, C.E. Jahr, Comparison of coupled and uncoupled currents during glutamate uptake by GLT-1 transporters, J. Neurosci. 22 (2002) 10153–10162.
[33] L. Chu, J.L. Greenstein, R.L. Winslow, Modeling Na^+-Ca^{2+} exchange in the heart: allosteric activation, spatial localization, sparks and excitation-contraction coupling, J. Mol. Cell. Cardiol. 99 (2016) 174–187.
[34] K.P. Lehre, N.C. Danbolt, The number of glutamate transporter subtype molecules at glutamatergic synapses: chemical and stereological quantification in young adult rat brain, J. Neurosci. 18 (1998) 8751–8757.
[35] S. Kirischuk, V. Parpura, A. Verkhratsky, Sodium dynamics: another key to astroglial excitability? Trends Neurosci. 35 (2012) 497–506.
[36] C.R. Rose, A. Verkhratsky, Principles of sodium homeostasis and sodium signalling in astroglia, Glia. 64 (2016) 1611–1127.
[37] R. Srinivasan, B.S. Huang, S. Venugopal, A.D. Johnston, H. Chai, H. Zeng, P. Golshani, B.S. Khakh, Ca(2+) signaling in astrocytes from Ip3r2(-/-) mice in brain slices and during startle responses in vivo, Nat. Neurosci. 18 (2015) 708–717.
[38] M. Bacigaluppi, G.L. Russo, L. Peruzzotti-Jametti, S. Rossi, S. Sandrone, E. Butti, R. De Ceglia, A. Bergamaschi, C. Motta, M. Gallizioli, V. Studer, E. Colombo, C. Farina, G. Comi, L.S. Politi, L. Muzio, C. Villani, R.W. Invernizzi, D.M. Hermann, D. Centonze, G. Martino, Neural stem cell transplantation induces stroke recovery by upregulating glutamate transporter GLT-1 in astrocytes, J. Neurosci. 36 (2016) 10529–10544.
[39] F. Boscia, G. Begum, G. Pignataro, R. Sirabella, O. Cuomo, A. Casamassa, D. Sun, L. Annunziato, Glial Na^+-dependent ion transporters in pathophysiological conditions, Glia 64 (2016) 1677–1697.
[40] A. Dvorzhak, N. Helassa, K. Török, D. Schmitz, R. Grantyn, Single synapse indicators of impaired glutamate clearance derived from fast $iGlu_u$ imaging of cortical afferents in the striatum of normal and Huntington (Q175) Mice, J. Neurosci. 39 (2019) 3970–3982.
[41] A. Dvorzhak, T. Vagner, K. Kirmse, R. Grantyn, Functional indicators of glutamate transport in single striatal astrocytes and the influence of Kir4.1 in normal and

Huntington mice, J. Neurosci. 36 (2016) 4959–4975.
[42] M. Maiolino, P. Castaldo, V. Lariccia, S. Piccirillo, S. Amoroso, S. Magi, Essential role of the Na^+-Ca^{2+} exchanger (NCX) in glutamate-enhanced cell survival in cardiac cells exposed to hypoxia/reoxygenation, Sci. Rep. 7 (2017) 13073.
[43] C. Murphy-Royal, J.P. Dupuis, J.A. Varela, A. Panatier, B. Pinson, J. Baufreton, L. Groc, S.H.R. Oliet, Surface diffusion of astrocytic glutamate transporters shapes synaptic transmission, Nat. Neurosci. 18 (2015) 219–226.
[44] A. Nicaise, C. Marneffe, J. Bouchat, J. Gilloteaux, Osmotic demyelination: from an oligodendrocyte to an astrocyte perspective, Int. J. Mol. Sci. 20 (2019) 1124.
[45] G. Pignataro, R. Sirabella, S. Anzilotti, G. Di Renzo, L. Annunziato, Does Na^+/Ca^{2+} exchanger, NCX, Represent a new druggable target in stroke intervention? Transl. Stroke Res. 5 (2014) 145–155.
[46] T. Rodrigues, G.N.N. Estevez, I.L.D.S. Tersariol, Na^+/Ca^{2+} exchangers: unexploited opportunities for cancer therapy? Biochem. Pharmacol. 163 (2019) 357–361.
[47] J.D. Rothstein, S. Patel, M.R. Regan, C. Haenggeli, Y.H. Huang, D.E. Bergles, L. Jin, M. Dykes-Hoberg, S. Vidensky, D.S. Chung, S.V. Toan, L.I. Bruijn, Z.Z. Su, P. Gupta, P.B. Fisher, Beta-lactam antibiotics offer neuroprotection by increasing glutamate transporter expression, Nature 433 (2005) 73–77.
[48] R. Sogaard, L. Borre, T.H. Braunstein, K.L. Madsen, N. MacAulay, Functional modulation of the glutamate transporter variant GLT1b by the PDZ domain protein PICK1, J. Biol. Chem. 288 (2013) 20195–20207.
[49] K. Takahashi, Q. Kong, Y. Lin, N. Stouffer, D.A. Schulte, L. Lai, Q. Liu, Chang L.-C, S. Dominguez, X. Xing, G.D. Cuny, K.J. Hodgetts, M.A. Glicksman, C.-L.G. Lin, Restored glial glutamate transporter EAAT2 function as a potential therapeutic approach for Alzheimer's disease, J. Exp. Med. 212 (2015) 319–332.
[50] X. Tong, Y. Ao, G.C. Faas, S.E. Nwaobi, J. Xu, M.D. Haustein, M.A. Anderson, I. Mody, M.L. Olsen, M.V. Sofroniew, B.S. Khakh, Astrocyte Kir4.1 ion channel deficits contribute to neuronal dysfunction in Huntington's disease model mice, Nat. Neurosci. 17 (2014) 694–703.
[51] A. Verkhratsky, R. Zorec, V. Parpura, Stratification of astrocytes in healthy and diseased brain, Brain Pathol. 27 (2017) 629–644.
[52] A.M. Wójtowicz, A. Dvorzhak, M. Semtner, R. Grantyn, Reduced tonic inhibition in striatal output neurons from Huntington mice due to loss of astrocytic GABA release through GAT-3, Front. Neural Circuits 7 (2013) 188.
[53] M. Charvériat, C.C. Naus, L. Leybaert, J.C. Sáez, C. Giaume, Connexin-dependent neuroglial networking as a new therapeutic target, Front. Cell. Neurosci. 11 (2017) 174.
[54] S. Guerra-Gomes, N. Sousa, L. Pinto, J.F. Oliveira, Functional roles of astrocyte calcium elevations: from synapses to behavior, Front. Cell. Neurosci. 11 (2017) 427.
[55] K. Heuser, C.G. Nome, K.H. Pettersen, K.S. Åbjørsbråten, V. Jensen, W. Tang, R. Sprengel, E. Taubøll, E.A. Nagelhus, R. Enger, Ca^{2+} signals in astrocytes facilitate spread of epileptiform activity, Cereb. Cortex 28 (2018) 4036–4048.
[56] O. Kékesi, E. Ioja, Z. Szabo, J. Kardos, L. Heja, Recurrent seizure-like events are associated with coupled astroglial synchronization, Front. Cell. Neurosci. 9 (2015) 215.
[57] L. Leybaert, M.J. Sanderson, Intercellular Ca^{2+} waves: mechanisms and function, Physiol. Rev. 92 (2012) 1359–1392.
[58] R. Schulz, P.M. Görge, A. Görbe, P. Ferdinandy, P.D. Lampe, L. Leybaert, Connexin 43 is an emerging therapeutic target in ischemia/reperfusion injury, cardioprotection and neuroprotection, Pharmacol. Ther. 153 (2015) 90–106.
[59] N. Vardjan, V. Parpura, R. Zorec, Loose excitation-secretion coupling in astrocytes, Glia 64 (2016) 655–667.
[60] R. Vincze, M. Péter, Z. Szabó, J. Kardos, L. Héja, Z. Kovács, Connexin 43 differentially regulates epileptiform activity in models of convulsive and non-convulsive epilepsies, Front. Cell. Neurosci. 13 (2019) 173.